# *Lamellipodial Versus Filopodial Mode of the Actin Nanomachinery: Pivotal Role of the Filament Barbed End*

Cell, Vol. 118, 363–373, August 6, 2004, Copyright ©2004 by Cell Press

# Lamellipodial Versus Filopodial Mode of the Actin Nanomachinery: Pivotal Role of the Filament Barbed End

**Marisan R. Mejillano,[1] Shin-ichiro Kojima,[1] Derek Anthony Applewhite,[1] Frank B. Gertler,[2] Tatyana M. Svitkina,[3] and Gary G. Borisy[1,*]**
[1]Department of Cell and Molecular Biology
Feinberg School of Medicine
Northwestern University
303 E. Chicago Avenue
Chicago, Illinois 60611
[2]Department of Biology
Massachusetts Institute of Technology
Cambridge, Massachusetts 02139
[3]Department of Biology
University of Pennsylvania
Philadelphia, Pennsylvania 19104

## Summary

**Understanding how a particular cell type expresses the lamellipodial or filopodial form of the actin machinery is essential to understanding a cell's functional interactions. To determine how a cell "chooses" among these alternative modes of "molecular hardware," we tested the role of key proteins that affect actin filament barbed ends. Depletion of capping protein (CP) by short hairpin RNA (shRNA) caused loss of lamellipodia and explosive formation of filopodia. The knockdown phenotype was rescued by a CP mutant refractory to shRNA, but not by another barbed-end capper, gelsolin, demonstrating that the phenotype was specific for CP. In Ena/VASP deficient cells, CP depletion resulted in ruffling instead of filopodia. We propose a model for selection of lamellipodial versus filopodial organization in which CP is a negative regulator of filopodia formation and Ena/VASP has recruiting/activating functions downstream of actin filament elongation in addition to its previously suggested anticapping and antibranching activities.**

## Introduction

Two alternate forms of actin machinery coexist at the leading edge of most motile cells: lamellipodia which seem designed for persistent protrusion over a surface, and filopodia which appear to perform sensory and exploratory functions to steer cells depending on cues from the environment. Although lamellipodia have been investigated since the pioneering work of Abercrombie (1970), filopodia have emerged in recent years as important in a broad range of cell biological processes, including epithelial sheet closure in development, wound healing, neuronal path finding, immune cell function, cell invasion, and metastasis of cancer cells (Jacinto and Wolpert, 2001; Rorth, 2003).

Although most cells in culture express both lamellipodia and filopodia, some cells, such as keratocytes or neutrophils, express lamellipodia almost exclusively; others, such as dendritic cells or the growth cones of neurons, are dominated by filopodia. Thus, understanding how a particular cell type expresses one or the other form of the actin machinery is essential to understanding a cell's functional interactions. An emerging general issue in cell biology is how the nanomachinery of a cell self-organizes. In the context of the actin machinery for protrusive motility, this issue may be expressed as how the cell "chooses" between lamellipodial and filopodial modes of the "molecular hardware."

Two models have been proposed to account for the formation of actin-based protrusions in crawling cells: the dendritic nucleation model for lamellipodia (Mullins et al., 1998; Pollard and Borisy, 2003; Svitkina and Borisy, 1999) and the convergent elongation model for filopodia (Svitkina et al., 2003). In lamellipodia, branched nucleation of actin is driven by activation of the Arp2/3 complex, followed by filament elongation and barbed-end capping. The necessity for barbed-end capping in lamellipodial protrusion is counterintuitive since it terminates filament elongation, which is the driving force for motility (Pollard and Borisy, 2003). However, capping is necessary to keep filaments short and their number constant (Borisy and Svitkina, 2000; Carlier, 1998; Cooper and Schafer, 2000). In filopodia, both branching and capping need to be prevented to allow continuous elongation of parallel filaments at their tip (Katoh et al., 1999; Mallavarapu and Mitchison, 1999). In the convergent-elongation model (Svitkina et al., 2003; Vignjevic et al., 2003), filopodia are initiated from a dendritic network by action of a tip complex that protects filaments against capping allowing for their elongation coordinated with a bundling activity. Thus, these models focus on the elongation status of the actin filament barbed end as a crucial determinant of whether lamellipodial or filopodial protrusion results.

The elongation status of the barbed end may be considered as the net result of an interplay between capping and anti-capping activities. Capping protein (CP), an $\alpha/\beta$ heterodimer ($M_r$ $\alpha$ ~36 kDa; $\beta$ ~32 kDa) (Schafer et al., 1994) is considered the major barbed-end terminator during cell motility because it (a) has high affinity ($K_d$ = 0.1–1 nM) for actin filament barbed ends in vitro, (b) is ubiquitous in eukaryotes (Cooper et al., 1999), (c) is enriched in lamellipodia (Schafer et al., 1998), and (d) supports in vitro reconstituted bacterial comet tail motility (Loisel et al., 1999). Furthermore, loss of function or null mutations in genetic systems such as yeast (Amatruda et al., 1990, 1992; Sizonenko et al., 1996), *Drosophila* (Hopmann et al., 1996), and *Dictyostelium* (Hug et al., 1995) resulted in aberrant actin architecture. The Ena/VASP family of proteins have been shown to promote formation of longer and less branched actin filaments at the leading edge in vivo and to be present at the tips of filopodia (Bear et al., 2002). Thus, Ena/VASP have been considered to have anticapping activity and are therefore candidate effectors controlling barbed ends.

Models of lamellipodial and filopodial formation predict barbed-end capping lies at the fork in the road of these two pathways. Consequently, we tested whether

*Correspondence: g-borisy@northwestern.edu

proteins that affect actin filament barbed ends could determine which form of the actin machinery was selected. Experiments were carried out in highly motile cells expressing both protrusive structures to facilitate observation of alternate phenotypes. Specifically, we tested whether barbed-end capping by CP and anticapping by Ena/VASP proteins are key elements in the mechanism of the lamellipodial/filopodial transition. We report that CP depletion resulted in inhibition of lamellipodia and explosive formation of filopodia. Contrary to expectations based on only an anticapping role for Ena/VASP, CP depletion in the absence of Ena/VASP resulted in ruffling, not filopodia. We propose a model for regulation of the lamellipodial/filopodial transition in which CP is a negative regulator of filopodia formation and Ena/VASP has functions downstream of actin filament elongation in addition to its previously suggested anticapping activity (Bear et al., 2002).

## Results

### Strategy of CP Depletion and Rescue

Targeted depletion of CP by RNA interference was used here as an approach to investigate CP function in cultured cells. For this purpose, we prepared a hairpin siRNA expression vector with a GFP marker (Kojima et al., 2004) for the added advantage of easier detection and sorting of expressing cells. Vertebrates have three α isoforms, each encoded by a separate gene, and three β isoforms produced from a single gene by alternative splicing. β1 is found mostly in muscle (at the Z-line), β2 is widespread in nonmuscle cells (Schafer et al., 1994), and β3 is present exclusively in male germ cells (von Bulow et al., 1997). Two different 19-nucleotide targeting sequences (T1, T2; Figure 1A) were selected that were common to mouse and rat CP β1 and β2 mRNA-coding regions while not having significant homology to any other known genes in the mouse or rat database as determined by BLAST search (NCBI). Since functional CP exists only as a heterodimer, silencing of the β-subunit was predicted to lead to functional loss of capping activity (Amatruda et al., 1992; Schafer et al., 1992).

Controls for the specificity of silencing involved two approaches: expression of siRNAs with mismatching nucleotides and rescue of the knockdown phenotype by a CP gene that was refractory to silencing. siRNAs are known to be highly specific and modification of only one or two base pairs in the target sequence is enough to abrogate silencing. Therefore, we designed hairpin constructs, T1* and T2*, identical to T1 and T2, respectively, except for two base pair mismatches in the target sequence (Figure 1A). CP β2 cDNAs refractory to silencing were designed by introducing mutations in the third nucleotide position of two codons (identical to those in T1* and T2*) that did not affect the amino acid sequence. These silent mutations would produce mutant mRNAs refractory to RNAi, thus permitting expression of wild-type protein that could support rescue. Empty pG-Super vector that expresses just the soluble GFP marker was used as a control for transfection and GFP expression.

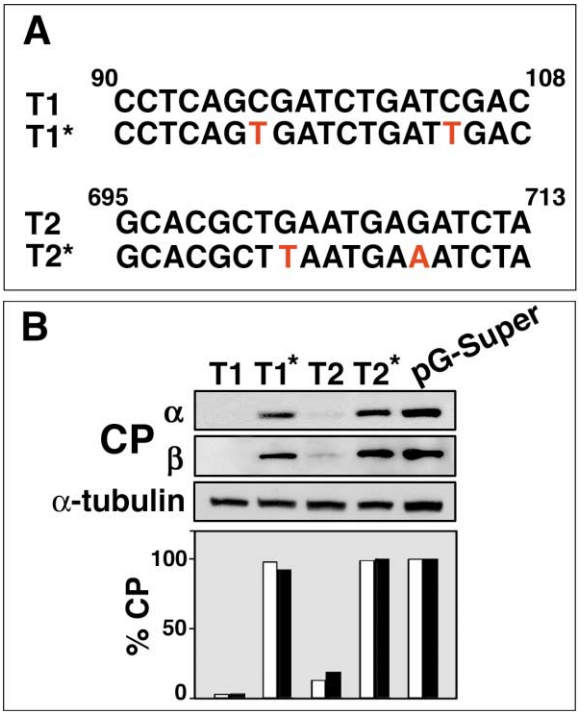


Figure 1. Expression of Hairpin siRNA Results in CP Depletion in B16F1 Cells

(A) Target sequences, T1 and T2, selected for mouse and rat β1 and β2 mRNA. Control mismatch target sequences, T1* and T2*, contain two nucleotide changes (red). Nucleotide numbers from start codon of mouse β2 subunit are indicated.

(B) Immunoblots and densitometry results of lysates prepared from FACS-purified cell populations five days after transfection of shRNA constructs. The same blot was first probed with CPα antibody (α), then with the pan CPβ (R22) antibody (β); α-tubulin served as loading control. Bar chart shows relative protein levels from densitometry analysis of the immunoblots shown above. Protein amount from lysates expressing pG-Super empty vector was assigned 100%. CPα, white bars; CPβ black bars. Knockdown of CP β subunit also resulted in loss of α subunit.

### CP Depletion in B16F1 Cells

Detailed analysis of the CP knockdown phenotype was performed using the mouse melanoma B16F1 cell line because these cells are highly motile and express lamellipodia and filopodia. Cells expressing T1- or T2 shRNA were surprisingly viable and could be grown in culture for more than a week. GFP-expressing cells were collected by fluorescence-activated cell sorting (FACS) one day after transfection (>99% GFP positive in the sorted population) and analyzed 3–5 days later. Microscopic inspection of the sorted cell population showed that >90% of cells were still GFP positive after five days. Immunoblotting confirmed silencing at the protein level (Figure 1B) with the average reduction in CP being 95% for T1 and 90% for T2. Control transfections with T1* and T2* hairpin constructs did not result in decreased CP amounts compared to transfection with GFP alone, demonstrating that knockdown achieved by T1 or T2 siRNA was specific. Consistent with earlier studies that CP is stable only as a heterodimer (Amatruda et al., 1992; Schafer et al., 1992), knockdown of the β-subunit

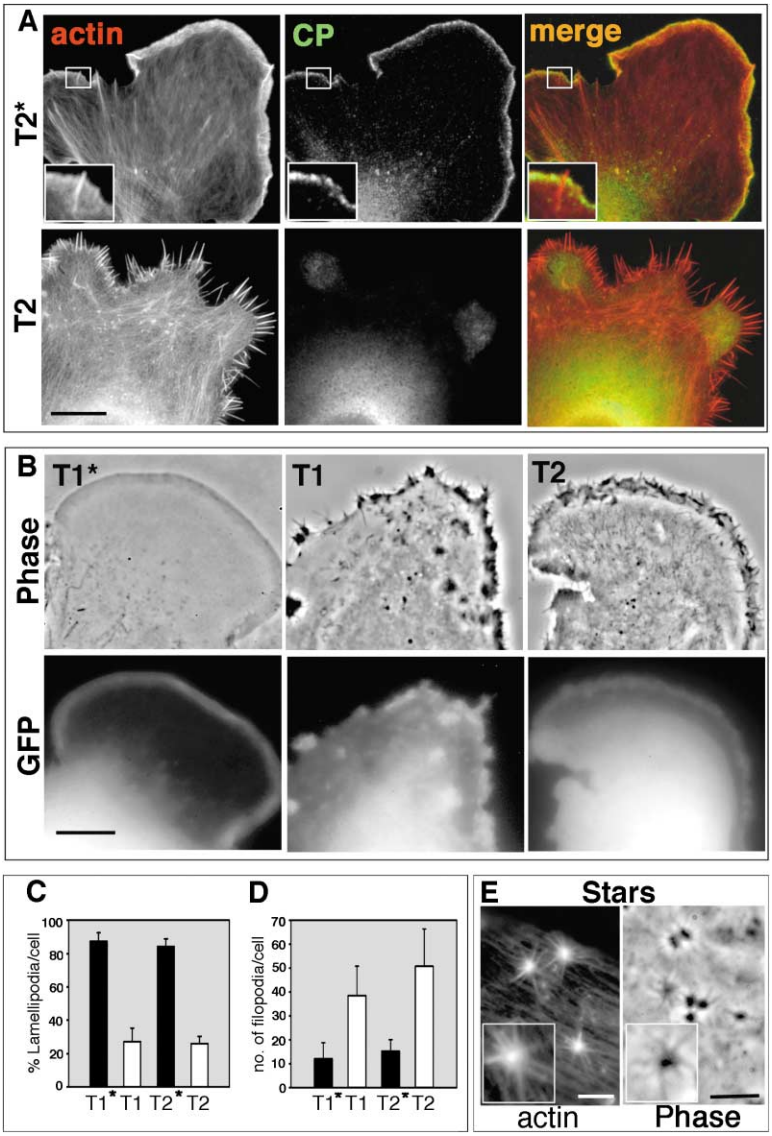


Figure 2. Phenotype of CP Knockdown B16F1 Cells

(A) Distribution of actin revealed by phalloidin staining (left column) and CP revealed by R26 antibody (middle column) in fixed cells expressing pG-Super-T2* (upper row) or pG-Super-T2 (lower row) for 5 days. Right column shows merged images. Boxed regions are enlarged in insets. T2*-expressing cell exhibits normal morphology with CP localized at extreme leading edge of lamellipodia and excluded from filopodia (insets). T2-expressing cell displays numerous filopodia, reduction of lamellipodia, and no CP staining at the cell periphery. Residual diffuse fluorescence in thick cell regions is attributed to nonspecific binding of secondary antibody. Scale bar is equal to 10 μm.

(B) Phase contrast (upper row) and GFP fluorescence (lower row) images of live control (T1*) and knockdown (T1 and T2) cells four days after transfection with respective pG-Super constructs demonstrate increase in lamella density (phase) and thickness (GFP) after CP knockdown. Scale bar is equal to 10 μm.

(C and D) Quantification of lamellipodia reduction (C) or filopodia enrichment (D) after CP knockdown. Bars represent average % of cell perimeter occupied by lamellipodial network (C) or average number of filopodia (D) in phalloidin-stained cells transfected with indicated shRNA constructs (n = 16–20 cells). CP induced changes were significant ($p < 0.0001$) for both lamellipodia and filopodia as determined by Student's t test.

(E) Stars formed at ventral surface of knockdown cells detected by phalloidin staining (left) and by phase contrast microscopy (right). Insets show enlarged examples. Scale bar is equal to 5 μm.

also resulted in comparable depletion of the α-subunit (Figure 1B).

CP depletion was assayed at the cellular level by immunostaining with CP antibody. Phalloidin was used to visualize actin in the same cells. CP in control cells (Figure 2A, upper row) was enriched at the extreme leading edge of lamellipodia and was excluded from filopodia, as demonstrated previously (Svitkina et al., 2003). In knockdown cells (Figure 2A, lower row), CP labeling was abolished at the leading edge, consistent with reduction in CP protein levels shown by immunoblotting.

### Attenuation of Lamellipodia Formation by CP Knockdown in B16F1 Cells

Control B16F1 cells (nontransfected cells, cells expressing GFP alone or T1* and T2* constructs, Figure 2A, upper row), growing on laminin-coated glass protruded large thin lamella with broad actin-rich lamellipodia at their leading edge, and a variable number of filopodia partially or completely embedded in the lamellipodia. However, in knockdown cells, lamellipodia were significantly attenuated. CP depletion caused cells to lose their characteristic flat, thin morphology with a convex leading edge and the cell perimeter lost its smooth outline. The whole leading lamella extending from the cell edge toward the cell body appeared much denser in phase contrast images (Figure 2B, upper row); in fluorescence images, they had higher intensity of soluble GFP because of increased thickness (Figure 2B, lower row). Phalloidin staining revealed a significant decrease in the lamellipodial actin network and an increase in actin staining in deeper lamellar regions (Figure 2A, lower row) compared to cells expressing GFP alone or mismatched hairpin constructs (Figure 2A, upper row). Morphometric analysis showed a 3–4-fold decrease in the percentage of lamellipodial perimeter associated with diffuse actin network (Figure 2C), whereas overall cell shape and spread area were not dramatically changed.

Attenuation of lamellipodia was confirmed by dimin-

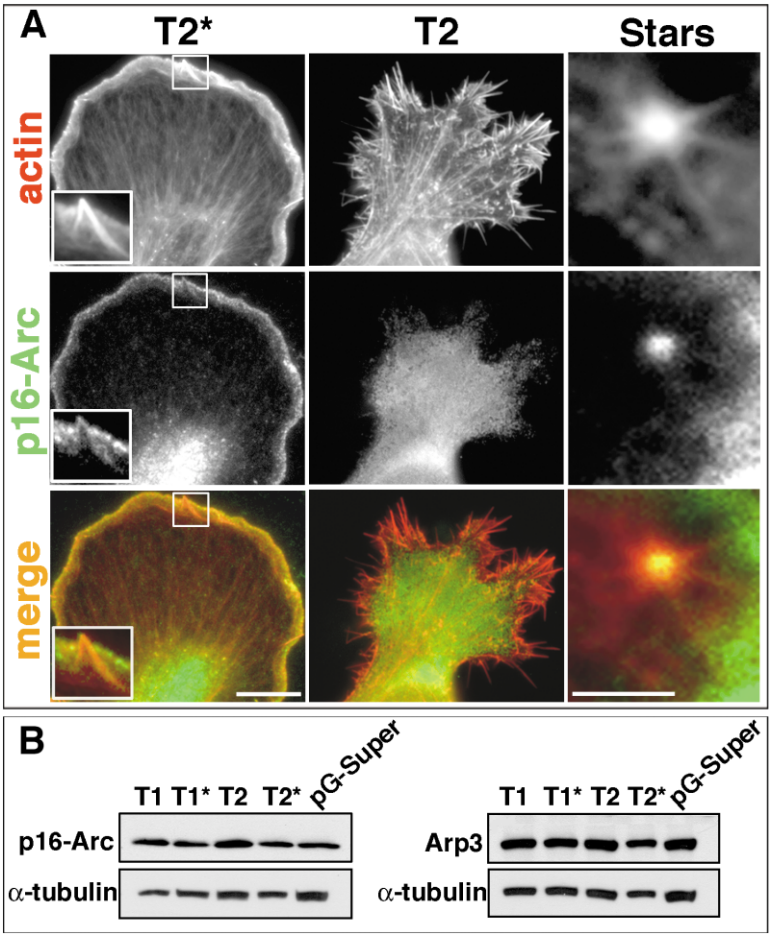


Figure 3. Displacement of the Arp2/3 Complex in Knockdown B16F1 Cells

(A) Distribution of Arp2/3 complex revealed by p16-Arc antibody (middle row) and actin by phalloidin staining (top row) in fixed cells expressing pG-Super-T2* (left column) or pG-Super-T2 (middle column) for five days. Bottom row shows merged images. Boxed regions are enlarged in insets. T2*-expressing cell exhibits normal morphology with Arp2/3 complex localized throughout the lamellipodium and excluded from filopodia (insets). T2-expressing cell displays numerous filopodia and is almost devoid of lamellipodia, with Arp2/3 labeling absent from periphery but with some diffuse staining observed in the cytoplasm. Scale bar is equal to 10 μm. Right column shows Arp2/3 and actin distribution in stars, with Arp2/3 localized only at the center. Scale bar is equal to 5 μm.

(B) Immunoblots performed five days after shRNA transfection with indicated constructs and probed with either p16 (left) or Arp3 (right) antibody indicate no decrease in Arp2/3 complex protein levels after CP knockdown. α-Tubulin antibody probing was used as loading control.

ished Arp2/3 staining at the leading edge (Figure 3A). In control cells, Arp2/3 complex was enriched in lamellipodia and substantially colocalized with lamellipodial actin but was significantly diminished at the perimeter of knockdown cells. However, protein levels of two different Arp2/3 complex subunits (p16 and Arp3) were unchanged as shown by Western blotting (Figure 3B), indicating that lamellipodial attenuation was not due to a reduction in overall cellular levels of the Arp2/3 complex. Thus, lamellipodial attenuation by CP depletion was accompanied by a redistribution of the Arp2/3 complex so that it was no longer enriched at the cell perimeter.

### Enhanced Filopodia Formation in CP Knockdown B16F1 Cells

Concomitantly with lamellipodia attenuation, CP depletion caused explosive formation of filopodia (Figure 2A, lower row). Increased filopodia were apparent as early as three days after siRNA-plasmid transfection and the increase was confirmed by quantitative analysis (Figure 2D). Filopodia formation in knockdown cells occurred not only at the cell edges, but also on the dorsal cell surface. Since it was feasible to count only those filopodia originating from cell edges, the real magnitude of enhanced filopodia formation may be greater than estimated.

In addition to peripheral and dorsal filopodia, star-like structures which could be identified both in phase-contrast images and after phalloidin staining (Figure 2E) were present at the ventral cell surface of 60 ± 15% (100 cells, n = 3 experiments) of knockdown cells. These "stars" were found in lamellar and perinuclear regions. They consisted of actin-containing spikes radiating from a center brightly stained with phalloidin.

A hallmark of genuine filopodia is enrichment of fascin, an actin bundling protein, along the length of filopodia (Kureishy et al., 2002), and VASP, a barbed-end binding protein (Bear et al., 2002), at their tips (Lanier et al., 1999; Rottner et al., 1999). Cellular levels of both proteins remained unchanged after CP knockdown in B16F1 cells as determined by immunoblotting (data not shown). By immunofluorescence, all lateral, dorsal, or ventral spikes showed fascin staining along their lengths (Figure 4A, upper row) and VASP staining at their tips (Figure 4B, upper row). A lamellipodial marker, Arp2/3 complex is usually depleted from filopodial bundles (Svitkina and Borisy, 1999). Consistent with this, we found that all filopodia induced by CP knockdown lacked Arp2/3 complex (Figure 3A), including the ventral stars, which were positive for Arp2/3 complex at their center but not along their radii (Figure 3A, right column). The staining pattern of ventral stars was similar to the filopodial-like bundles reconstructed in vitro from beads coated with Arp2/3 activators (Vignjevic et al., 2003). Thus, molecular marker

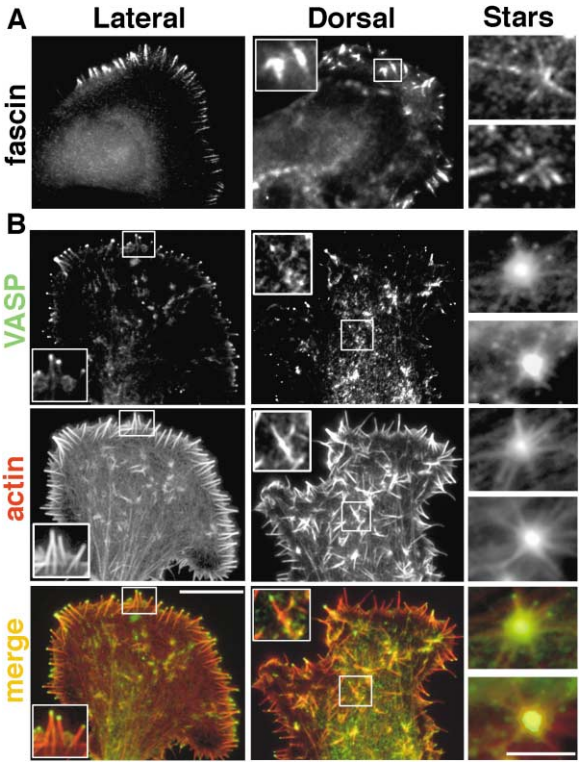


Figure 4. Filopodial Markers Have Normal Distribution in Filopodia Induced by CP Knockdown.

Knockdown B16F1 cells expressing pG-Super-T1 construct for four days show numerous lateral filopodia (left column), dorsal filopodia (middle column) and ventral stars (right column).
(A) Antibody staining reveals fascin along the length of filopodia.
(B) VASP (upper row) and actin (middle row) costaining reveals VASP at the filopodial tips. Merged images of VASP and actin are shown in bottom row. Boxed regions are enlarged in insets. Scale bars are equal to 10 μm (left and middle columns) and 5 μm (right column).

analyses confirmed that the spikes and stars induced by CP depletion were similar to filopodia.

Electron microscopy was carried out to evaluate the phenotype of CP knockdown in B16F1 cells in more detail. Low magnification views showed that control cells contained few filopodia that were restricted to the cell periphery (Figure 5A), whereas CP knockdown cells showed abundant filopodial-like protrusions around the cell perimeter and on the dorsal surface (Figure 5C), which significantly varied in thickness and appeared emerging from the surrounding network. In addition, the leading lamella of knockdown cells was filled with a dense actin filament network, which contrasted with a rather sparse lamella cytoskeleton in control cells and suggested increased actin filament assembly away from the leading edge after CP depletion. High resolution analysis demonstrated that similar to normal filopodia (Figure 5B), lateral (Figure 5D) and dorsal (inset in Figure 5C) protrusions in CP knockdown cells contained bundles of long unbranched actin filaments that extended almost the entire length of the bundle. Thus, EM data are also consistent with the idea that CP knockdown-induced genuine filopodia with proper structural organization.

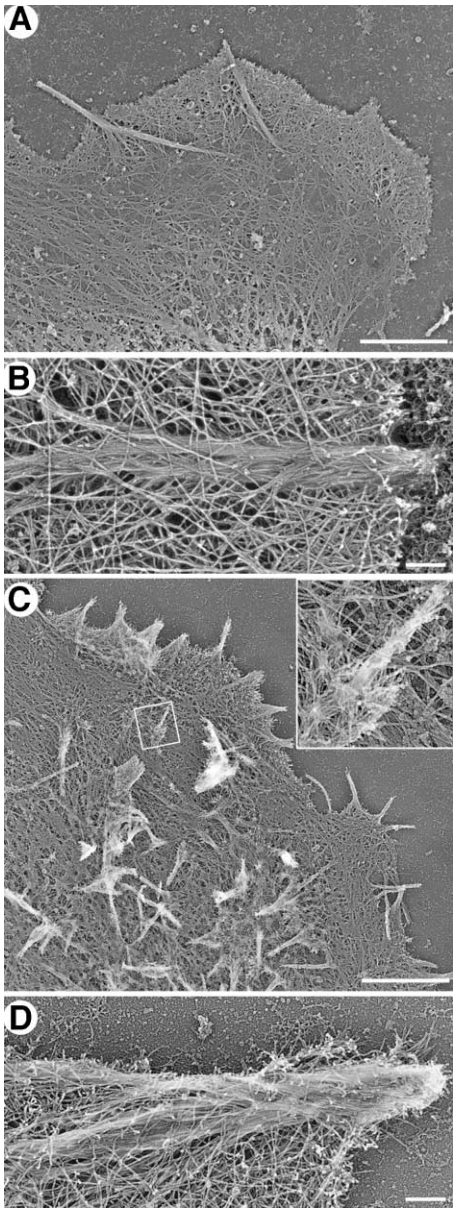


Figure 5. Structural Organization of Filopodia in B16F1 Cells

(A and B) Control cells. Platinum replica EM shows few peripherally located filopodia embedded into lamellipodial network. Deeper cytoplasm shows sparser filament network.
(C and D) CP knockdown cells. Abundant filopodia are apparent at both leading edge and dorsal surface. Deeper cytoplasm shows dense filament network. High magnification images of control (B) and CP knockdown (D) filopodia show their similar structural organization. Enlarged image of boxed region in (C) shows that dorsal filopodium contains a bundle of parallel filaments. Scale bars are equal to 5 μm (A, C) and 1 μm (B, D).

Kinetic analysis was performed to determine the dynamics of induced filopodia and to evaluate the effect of CP knockdown on the protrusion of the leading edge (See Supplemental Movies S1 and S2 available at http://www.cell.com/cgi/content/full/118/3/363/DC1). Time lapse movies of knockdown cells demonstrated that induced filopodia displayed normal dynamic features: protrusive, retractile, and sweeping motility. Dorsal filo-

podia were not formed as a result of retrograde translocation but were formed de novo. When behavior of the leading edge was analyzed using kymographs, control cells displayed smooth and persistent protrusion for long periods of time, whereas CP-depleted cells displayed erratic protrusion-withdrawal behavior with no obvious coordination between adjacent regions of the leading edge (Supplemental Figure S1, Supplemental Movies S1 and S2 available on *Cell* website). As a result, knockdown cells demonstrated significant decrease in net protrusion. The average rate of leading edge advance in CP-depleted cells (0.32 $\pm$ 0.36 $\mu$m/min) was 2.0$\times$ lower as compared to their mismatch controls (0.64 $\pm$ 0.41 $\mu$m/min) (4 s frame rate; 5 min observation period; 42 kymographs; 10 cells, $p < 0.001$).

### Rescue of Knockdown Phenotype

We attempted to rescue CP depleted cells by expressing CP refractory to the siRNA. Successful rescue would not only provide a stringent test for the specificity and reversibility of the knockdown phenotype; it would also test whether CP tagged with fluorescent protein could efficiently substitute for endogenous capping activity. We constructed CP$\beta$2 subunits containing silent mutations (T1*, T2*; Figure 1A). To monitor simultaneously knockdown and rescue constructs in transfected cells, CFP was substituted for GFP in the pG-Super T1 and T2 knockdown constructs, and the rescue constructs, T1*- and T2*-CP$\beta$2, were expressed as YFP-fusion proteins. Thus, CFP was taken as the indicator of knockdown and YFP the indicator of rescue. Cells were first transfected with knockdown constructs to allow phenotype development and on day 3 were transfected with one of the rescue constructs.

The phenotype of expressing cells 2–3 days after YFP-CP (T1* or T2*) transfection was analyzed by phase contrast and fluorescence microscopy. Most cells expressing both CFP and YFP (90%; n = 101) exhibited prominent flat, thin lamellipodia and distinct CP localization at the cell periphery, a phenotype characteristic of control cells (Figure 6A, *i*). These results also indicated that adding back the $\beta$-subunit by transfection of YFP-CP$\beta$ restored CP $\alpha$-subunit to normal cellular levels. In the same population, cells expressing only CFP (100%; n = 106) still showed the knockdown phenotype (Figure 6A, *ii*), characterized by abundant filopodia and thick, dense lamella. All YFP-only positive cells (n = 100) had normal CP localization at the leading edge indistinguishable from wild-type (Figure 6A, *iii*). Thus, expression of the rescue construct induced phenotypic reversion in the presence of inhibitory siRNA demonstrating specificity and lack of irreversible downstream effects of CP depletion. Rescue also established that CP tagged with derivatives of GFP could support normal capping function.

Next, we tested whether rescue could be achieved with another barbed-end capper, gelsolin, or whether the phenotype was indeed specific for CP. We confirmed that gelsolin is present in B16F1 melanoma cells by immunoblotting (data not shown). Immunofluorescence staining (Supplemental Figure S2 available on *Cell* website) showed that gelsolin is enriched in the lamellipodia, consistent with earlier studies (Chou et al., 2002). However, compared to CP, which is present mostly at the extreme leading edge (see Figures 2A and 6A), gelsolin distribution is broader, usually colocalizing with most of the lamellipodial actin network. For rescue experiments with gelsolin, we used the same strategy as for CP.

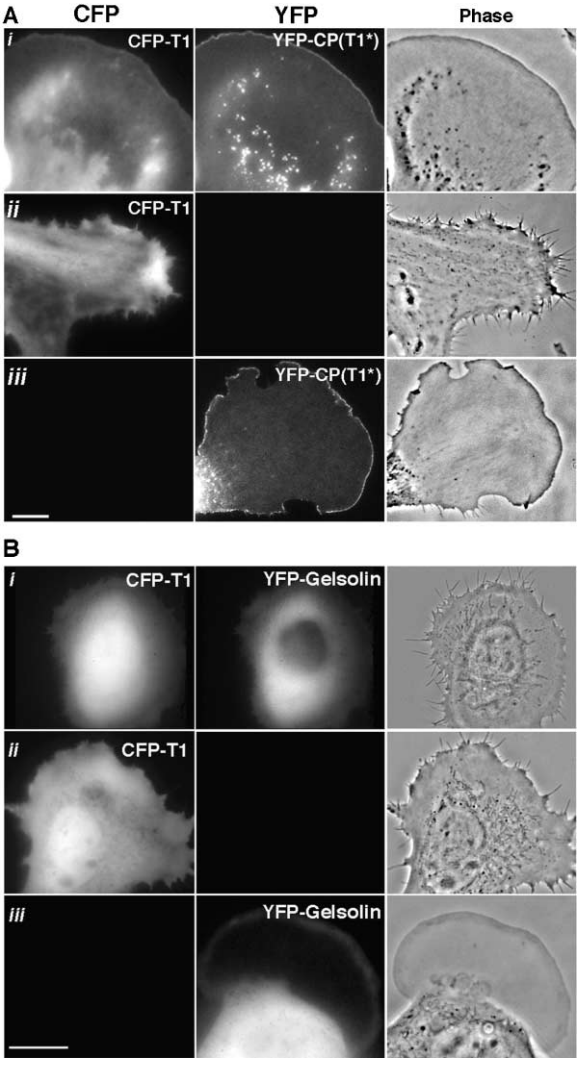


Figure 6. Rescue of CP Knockdown Phenotype in B16F1 Cells

(A) Rescue by CP refractory to siRNA. (*i*) Cell expressing both knockdown (CFP-T1 hairpin) construct (left) and rescue construct (YFP-CP(T1*)) refractory to siRNA (middle) shows wild-type phenotype with YFP-CP(T1*) localizing to the extreme leading edge as in normal cells. Phase image (right) shows flat and thin lamellipodial morphology indistinguishable from control cells. (*ii*) Cell expressing CFP-T1 hairpin (left), but not YFP-CP(T1*) (middle), displays characteristic of the knockdown phenotype with numerous spiky protrusions evident from the phase contrast image (right) and thick lamella as revealed by distribution of soluble CFP (left). (*iii*) Cell expressing silent mutant YFP-CP(T1*) (middle), but not CFP-T1 (left) shows wt distribution of CP at extreme leading edge. Corresponding phase contrast image (right) illustrates normal lamellipodial morphology. Scale bar is equal to 10 $\mu$m.

(B) Gelsolin does not rescue CP knockdown phenotype. (*i, ii*) Cells expressing both CFP-T1 and YFP-gelsolin (*i*), as well as cells expressing CFP-T1 alone (*ii*) still show abundant filopodia and diminished lamellipodia (phase images), characteristic of CP knockdown phenotype. (*iii*) Cell expressing only YFP-gelsolin displays gelsolin localization at the leading edge; corresponding phase image shows control phenotype. Scale bar is equal to 10 $\mu$m.

Results showed that 100% of cells expressing both CFP-T1 and YFP-gelsolin (n = 100) still showed the CP knockdown phenotype characterized by excessive filopodia and loss of lamellipodia, and that they were indistinguishable from cells expressing only CFP-T1 (Figure 6B, *i*, *ii*). Cells expressing only YFP-gelsolin exhibited gelsolin localization at the leading edge similar to that revealed by immunostaining. In phase contrast images, they displayed flat, thin lamellipodia, typical of control cells (Figure 6B, *iii*). These results show that another barbed-end-capping protein, gelsolin, does not functionally substitute for CP in these cells and suggests that the ability to control the lamellipodial/filopodial transition requires properties specific to CP.

### Generality of CP Knockdown Phenotype

To determine whether the phenotypic response of CP depletion reflects a general principle, we performed CP knockdown with shRNA in two other mammalian cell types: a murine fibroblast cell line, NIH3T3, and a rat fibroblast cell line, Rat2. Both cell types (Supplemental Figures S3 and S4 available on *Cell* website) displayed attenuation of lamellipodia and excessive formation of filopodia after CP depletion. As in B16F1 cells (see Figure 2A), control Rat2 and NIH3T3 cells expressing T2* construct showed that CP localized at the extreme leading edge and was excluded from filopodia; whereas in cells expressing the T2 knockdown construct, CP staining was abolished at the cell edge. Phalloidin staining and phase contrast microscopy revealed excessive filopodia and diminished (sometimes absent) lamellipodia in knockdown cells, a phenotype essentially similar to that of B16F1 cells depleted of CP.

### CP Knockdown in Cells Lacking Ena/VASP

CP activity in vivo may be affected by Ena/VASP family proteins that antagonize actin filament capping at the lamellipodial leading edge (Bear et al., 2002). Therefore, we performed CP depletion in $MV^{D7}$ murine fibroblasts lacking all endogenous Ena/VASP proteins (Bear et al., 2000). The phenotype of these cells was evaluated during spreading on laminin shortly (~30–45 min) after replating, during which time cells displayed extensive protrusive activity favorable for analysis. Control untransfected $MV^{D7}$ cells, as well as the derivative cells reexpressing Mena ($MV^{D7}$ EM), displayed a smooth, circular lamellipodium under these conditions (Figures 7A and 7B, upper rows). Less than 4% showed filopodia and these were few in number. Less than 10% of untransfected cells showed any ruffling and this was restricted to a small fraction of the cell perimeter. However, after expression of the T1 knockdown construct for five days, both cell types lost the smooth outline of their cell perimeter, but they did so in strikingly different ways (Figures 7A and 7B, lower rows). Most $MV^{D7}$ EM cells (73%), as expected, formed excessive filopodia (44.0 ± 2.0 per cell, n = 16 cells), whereas most $MV^{D7}$ cells (60%) exhibited extensive ruffling all along the cell perimeter, but not filopodia that were extremely rare (4.0 ± 0.2, n = 15; $p < 0.001$). These data confirm the results with the other cell lines that CP depletion compromised lamellipodia formation. In addition, they showed that CP depletion was not sufficient for filopodia formation, but that Ena/VASP was required as well.

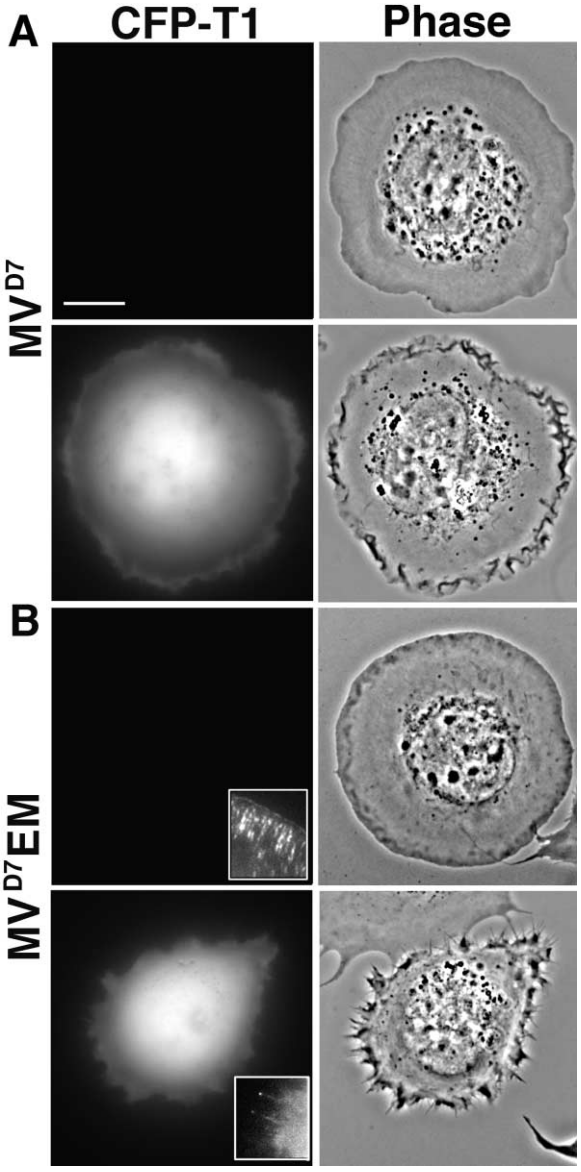


Figure 7. Phenotype of CP Depletion Depends on the Presence of Ena/VASP Proteins

(A) Ena/VASP-deficient $MV^{D7}$ cells spreading on laminin-coated glass display the smooth outline of the cell perimeter in control (upper image), but express numerous phase-dark ruffles after expressing CFP-T1 knockdown construct for five days (lower image) as observed by phase contrast microscopy of living cells.

(B) Similar to its parent cell line, untransfected $MV^{D7}$ reexpressing GFP-Mena cells ($MV^{D7}$ EM) (upper image), display smooth cell perimeter but show increased filopodial-like protrusions after expressing CFP-T1 knockdown construct for five days. Enlarged insets show GFP-Mena at extreme leading edge of control cell and at the tips of filopodia-like protrusions in knockdown cell. Scale bar is equal to 10 μm.

## Discussion

### CP-Dependent Control of the Lamellipodial/Filopodial Transition

The main features of the CP depletion phenotype were severe attenuation of lamellipodia and dramatic increase of filopodia. Lamellipodial attenuation was evi-

dent by the redistribution of Arp2/3 away from the cell perimeter, by loss of the normal dendritic brush near the leading edge and by appearance of a dense network of filaments throughout the cytoplasm, suggestive of uncontrolled polymerization. The loss of Arp2/3 at the cell perimeter needs to be explained because the overall cellular level of Arp2/3 was not affected by CP depletion and lack of capping is not predicted to interfere with branched nucleation. The simplest explanation is that the filopodial machinery, which excludes Arp2/3 complex along the length of actin bundles, becomes so dominant at the cell perimeter as to force the redistribution of Arp2/3. Another possibility is that the activities of CP and Arp2/3 complex are tightly coordinated in cells to produce a balanced dendritic network. Independent of the explanation of the redistribution of Arp2/3, these results indicate the positive requirement of CP for normal lamellipodial expression.

An even more striking result of CP knockdown was the extensive formation of filopodia, not just at the leading edge but also at the dorsal and ventral surfaces of cells. These results complement our previous findings in vitro (Vignjevic et al., 2003) showing that plastic beads coated with Arp2/3-activating proteins and placed into CP-depleted brain cytoplasmic extracts were not able to assemble comet tails, but assembled filament bundles in star-like configuration strikingly similar to ventral stars described here. The role of Arp2/3-activator coated beads in cells may be played by Arp2/3-rich cytoplasmic foci, which are abundant in B16F1 (Ballestrem et al., 1998) and other cell types (Schafer et al., 1998). Taken together, these results establish that CP is necessary for formation of dendritic arrays and that decreased CP concentrations favor transformation of the dendritic network into filopodial bundles.

Although a number of barbed-end cappers exist in cells (Schafer and Cooper, 1995), our data demonstrate that the filopodial phenotype was produced specifically by CP knockdown as it could be rescued by an RNAi-resistant mutant of CP, but not by gelsolin, another abundant ubiquitous barbed-end capper (Kwiatkowski, 1999). These findings agree with previous reports that gelsolin null cells show normal filopodial protrusion and display only a subtle phenotype with respect to their protrusive behavior (Azuma et al., 1998). Although filopodia were reported to be more abundant in gelsolin null neuronal growth cones as compared to wt, the increase was due to impaired retraction as opposed to increased protrusion (Lu et al., 1997).

Based on our current findings and work from other groups, we propose a model for the mechanism of regulation of lamellipodial versus filopodial protrusion by CP (Figure 8). In this model, Arp2/3-dependent dendritic nucleation of actin filaments is the starting point for formation of both actin filament arrays, but then the two pathways diverge depending on CP activity. We propose that when CP activity in the cell is high (Figure 8, upper images), newly nucleated filaments elongate for only a short period of time and become capped. To maintain protrusion, capped filaments are replaced by newly nucleated side branches produced by the Arp2/3 complex. This favors the formation of a dendritic lamellipodial network. In contrast, when activity of CP is low (Figure 8, lower images), filaments can elongate persistently and attain significant lengths. Other elements of the convergent elongation mechanism work on these preformed long filaments allowing their convergence and subsequent bundling to form filopodia.

### Control of Barbed-End Elongation

How is barbed-end elongation controlled? The mechanism of CP regulation is a long-standing issue that has not yet been resolved. In vitro, capping activity of CP can be inhibited by PIP2 micelles (Schafer et al., 1996), but it is not known whether such regulation takes place in vivo. No phosphorylation of CP has been reported (Schafer et al., 1994). Recently, two proteins interacting with CP have been identified. One of them, V-1, forms a stable complex with CP and inhibits its binding to actin filaments in vitro (Taoka et al., 2003). Another CP-interacting protein, CARMIL, was found in *Dictyostelium* and *Acanthamoeba* (Jung et al., 2001; Remmert et al., 2004), but it remains unknown whether it affects CP activity in vitro or in vivo.

Regulation of barbed-end elongation may involve proteins that antagonize capping. One group of such proteins is the Ena/VASP family. Ena/VASP proteins when targeted to the membrane promote formation of longer and less branched actin filaments at the leading edge and, conversely, depletion of Ena/VASP leads to shorter, more branched filaments (Bear et al., 2002). VASP is also enriched at filopodial tips (Lanier et al., 1999; Rottner et al., 1999), and accumulates at sites on the lamellipodial leading edge where filopodia emerge (Svitkina et al., 2003). Deficiency of Ena/VASP in *Dictyostelium* (Han et al., 2002) or neuronal cells (Lebrand et al., 2004) resulted in inhibition of filopodia, whereas overexpression or membrane targeting of VASP produced overabundant filopodia in *Dictyostelium*, as well as increased filopodial length and number in neurons. Ena/VASP proteins are known to be regulated by PKA/PKG-dependent phosphorylation (Kwiatkowski et al., 2003) at multiple phosphorylation sites. The conserved N-terminal Ser residue in vertebrate Ena/VASP proteins seems to be involved in fibroblast motility (Loureiro et al., 2002). Moreover, increased phosphorylation of this Ser in Mena in response to activation of PKA directly paralleled formation of filopodia in neurons (Lebrand et al., 2004). Thus, capping antagonists in their active form may serve as positive regulators of actin filament elongation and, therefore, filopodia formation. Evidence that the balance between capping and anticapping is critical to the "choice" of actin organization that dominates in a specific cell type or site comes from genetic analysis in *Drosophila* of microvilli and cleavage furrows (Grevengoed et al., 2003) and from immunoblot analysis of actin binding proteins in cell cultures showing low levels of CP and high levels of Ena/VASP in neurons as compared to fibroblasts (Strasser et al., 2004).

In addition to Ena/VASP, another group of proteins that antagonize capping has been identified recently, namely, formins. In vitro, formins nucleate actin filaments and remain associated with their growing barbed ends (Evangelista et al., 2003; Pruyne et al., 2002) while protecting them from capping (Evangelista et al., 2003; Harris et al., 2004; Moseley et al., 2004; Pruyne et al., 2002; Zigmond et al., 2003). Therefore, regulation of

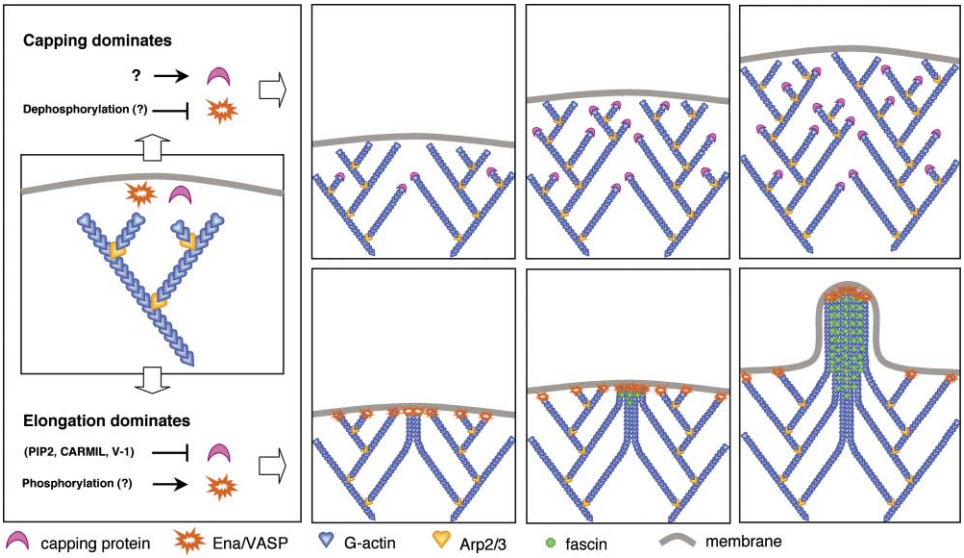


Figure 8. Model for Mechanism of Regulation of Lamellipodial Versus Filopodial Protrusion by Filament Capping

Box on left illustrates starting point for both types of protrusion and possible regulation of the proposed key players. Smaller boxes illustrate scenarios for lamellipodia (top) or filopodia (bottom) depending on capping activity: Top: when capping activity dominates either by activation of CP or inhibition of capping antagonists such as Ena/VASP, filaments elongate for a brief period before becoming capped and, as a consequence, these filaments are relatively short. To maintain protrusion, capped filaments are replaced by newly nucleated side branches produced by Arp2/3 complex, favoring the formation of a dominantly branched, lamellipodial network. Bottom: low capping activity resulting either from inhibition of CP or activation of proteins that promote anticapping and antibranching such as Ena/VASP, favor filament elongation leading to long and unbranched filaments, which converge and subsequently become bundled by fascin. Filopodia formation is therefore more predominant. CP inhibition may be mediated by PIP2, the CARMIL complex or the V-1 protein; Ena/VASP proteins may be activated by PKA/PKG-dependent phosphorylation.

formins also has the potential to influence the balance between filopodia and lamellipodia in cells.

### Control of Filopodia Formation

Why does CP depletion lead to filopodia formation and not just erratic protrusive behavior? According to the convergent elongation model, filament elongation represents only the first step of transition from the dendritic network to parallel bundles. Any missing or inactive element of the filopodial machinery downstream of filament elongation, such as filament bundling, would prevent filopodia formation and lead to uncontrolled polymerization. The fact that CP depletion led to explosive formation of filopodia indicates that the rest of the filopodia-making machinery was present in the cells and ready to go. This suggests that under normal conditions, control of the status of the actin filament barbed end at the leading edge serves as a crucial determinant of whether the lamellipodial or filopodial mode of the actin machinery is expressed.

*Drosophila* S2 cells treated with dsRNA against CP displayed excessive ruffling, but not filopodia (Rogers et al., 2003). Since filopodia were absent in S2 cells even in normal culture, an intrinsic deficiency of the filopodial machinery in this cell type is likely responsible for the different phenotype. The observed ruffling can be interpreted as a manifestation of inefficient protrusion resulting from long filaments buckling under the membrane.

What are the elements of the filopodial machinery necessary to complete filopodia formation after filament elongation is allowed? In this study, we showed that an Ena/VASP family member was essential for filopodia formation. Without Ena/VASP but with normal levels of CP, actin filaments were short and highly branched (Bear et al., 2002). Depleting CP in Ena/VASP deficient cells allowed for filament elongation. However, very few filopodia formed and cells switched to ruffling, similar to *Drosophila* S2 cells. Cells reexpressing Ena/VASP formed filopodia upon CP depletion. Thus, Ena/VASP proteins are not only capping antagonists (Bear et al., 2002), but also part of the filopodial machinery downstream of elongation (this study). Downsteam functions of Ena/VASP may involve establishing the functionality of the filopodial tip complex (Svitkina et al., 2003). Alternatively, Ena/VASP may participate in recruiting fascin or its activators, which are important for filament crosslinking, and therefore bundling (Vignjevic et al., 2003).

In summary, our analysis has demonstrated that key proteins, CP and Ena/VASP, play a critical role at the molecular "hardware" level of the actin protrusive machinery. They sit at a fork in the road of the dendritic-nucleation and convergent-elongation pathways for lamellipodia and filopodia formation, respectively. CP serves as a negative regulator of filopodia and a positive regulator of lamellipodia. Low levels of CP or high levels of its antagonists determine the extent of prolonged filament growth, which, if allowed, degrades the dendritic network, but allows for engagement of downstream machinery and filopodia formation. Ena/VASP proteins play an important role not only in terms of anticapping activity but also in the engagement of the downstream filopodial machinery. If absent or deficient,

actin filament growth results in ruffling, not filopodia formation. Although the full upstream pathway of regulation of cappers and anticappers remains to be elucidated, it is clear that such mechanisms exist and that they are likely complex and intertwined. The salient point of this study is that the elongation status of actin filament barbed ends determines the expression of the lamellipodial or filopodial mode of actin protrusion, contingent on the functionality of the downstream filopodial machinery.

## Experimental Procedures

### Expression Plasmids

pG-Super hairpin siRNA construct (Kojima et al., 2004) was based on the pSuper expression vector (Brummelkamp et al., 2002). pEGFP-CPβ2 was a gift from D. Schafer (University of Virginia). YFP-CPβ2 was obtained by transferring the CPβ2 cDNA into pEYFP-C1 (Clontech). Silent mutations in YFP-CP were introduced using the Quikchange site-directed mutagenesis kit II (Stratagene). pEYFP-gelsolin was constructed based on a cDNA fragment of human cytoplasmic gelsolin from pCMV-gelsolin, a gift from H.L. Yin (Univ. of Texas Southwestern Medical Center), and pEYFP-C1 with their HindIII-BamHI sites. To remove the 5′-untranslated region, a XhoI-NotI part in the 5′ region was replaced with a PCR-amplified fragment.

### Antibodies

The following rabbit polyclonal antibodies were obtained as gifts: CPβ2 C terminus (R26) and the pan-CPβ-subunit (R22) from D. Schafer; Arp3 from T. Uruno (Holland American Red Cross Laboratory); and gelsolin from H.L. Yin. CPα antibody was generated in rabbits against the peptide IESHQFQPKNFWNGRWRSEWK and affinity purified. Arp2/3 complex p16-Arc subunit antibody (Vignjevic et al., 2003) and VASP antibody (Bear et al., 2002) were described previously. The following antibodies were from commercial sources: fascin (DAKO Cytomation), α-tubulin (Sigma), secondary antibodies (Sigma, Jackson Laboratories). All other reagents were from Sigma unless indicated otherwise.

### Cell Culture and Microscopy

B16F1 mouse melanoma cells were provided by C. Ballestrem (Weizmann Institute of Science) and cultured as described previously (Ballestrem et al., 1998). NIH3T3 cells was purchased from ATCC and cultured in DMEM supplemented with 10% FBS. Rat2, $MV^{D7}$, and $MV^{D7}$ EM were cultured as described (Bear et al., 2000). Transient expression of proteins and shRNA was performed with FuGENE6 (Roche) according to manufacturer's recommendations. For live cell imaging, cells were transferred into L-15 medium or phenol red-free DMEM (Gibco) supplemented with 10% FBS.

Immunostaining was performed after cell extraction for 5 min with 1% Triton X-100 in PEM buffer (100 mM PIPES, [pH 6.9], 1 mM $MgCl_2$, 1 mM EGTA) containing 4% PEG, MW 40,000 (Serva) and 2 μM phalloidin, followed by fixation with 0.2% glutaraldehyde and quenching with $NaBH_4$. Texas red phalloidin (0.033 μM, Molecular Probes) was used for actin staining. Fascin staining was performed after methanol fixation of extracted cells. For VASP staining, cells were extracted and fixed simultaneously using a mixture of 0.5% Triton X-100 and 0.25% glutaraldehyde in PEM buffer. Primary antibody concentrations used were 5–50 μg/ml.

Light microscopy was performed using an inverted microscope (Eclipse TE2000 or Diaphot 300, Nikon) equipped with Plan 100× 1.3 NA objective and a back-illuminated cooled CCD camera (model CH250, Roper Scientific) driven by Metamorph imaging software (Universal Imaging Corp). For live imaging, cells were kept on the microscope stage at 37°C during observation.

Quantification of both lamellipodia and filopodia was done on fixed cells stained with Texas red phalloidin. Only spread cells containing a prominent leading lamella were chosen. For quantification of lamellipodia, Metamorph line function was used to trace and measure the whole-cell perimeter and cell perimeter with adjacent lamellipodial network. The fraction of cell perimeter occupied by lamellipodial network was used as a parameter for quantification. The number of filopodia per cell was determined by counting only filopodia crossing the cell edge and having fluorescence intensity 1.2× above background. Two researchers performed both measurements independently. Motility analysis was done using kymograph function in Metamorph. Statistical significance was determined by Student's t test. Graphs and statistical analysis were done using SigmaPlot software. Samples for platinum replica electron microscopy were processed as described (Svitkina and Borisy, 1998).

### Immunoblotting and Densitometry

Cells were lysed in buffer containing 10 mM Tris, [pH 7.5], 150 mM NaCl, 1% Triton X-100, 10% glycerol, and protease inhibitor tablet (Roche). Protein concentration of the lysates was determined using BCA reagent (Pierce). SDS-PAGE (4%–20% polyacrylamide) and immunoblotting were according to standard protocols. Densitometry analysis was performed using NIH Image software.

### Acknowledgments

We thank D. Schafer, T. Uruno, H. L. Yin, and C. Ballestrem for gifts of reagents; O. Chaga for technical assistance with phase contrast and electron microscopy; J. Peloquin for preparing CPα and p16 antibodies; A. Mongiu, O. Danciu, and G. Woodhead for help in preparing constructs; M. Paniagua for assistance in FACS; and S. Zigmond for critical reading of the manuscript. Supported by grants NIH GM62431 to G.G.B. and NIH GM58801 to F.B.G.

Received: October 29, 2003
Revised: June 14, 2004
Accepted: June 18, 2004
Published: August 5, 2004

### References

Abercrombie, M., Heaysman, J.E., and Pegrum, S.M. (1970). The locomotion of fibroblasts in culture. II. "Ruffling. Exp. Cell Res. *60*, 437–444.

Amatruda, J.F., Cannon, J.F., Tatchell, K., Hug, C., and Cooper, J.A. (1990). Disruption of the actin cytoskeleton in yeast capping protein mutants. Nature *344*, 352–354.

Amatruda, J.F., Gattermeir, D.J., Karpova, T.S., and Cooper, J.A. (1992). Effects of null mutations and overexpression of capping protein on morphogenesis, actin distribution and polarized secretion in yeast. J. Cell Biol. *119*, 1151–1162.

Azuma, T., Witke, W., Stossel, T.P., Hartwig, J.H., and Kwiatkowski, D.J. (1998). Gelsolin is a downstream effector of rac for fibroblast motility. EMBO J. *17*, 1362–1370.

Ballestrem, C., Wehrle-Haller, B., and Imhof, B.A. (1998). Actin dynamics in living mammalian cells. J. Cell Sci. *111*, 1649–1658.

Bear, J.E., Loureiro, J.J., Libova, I., Fassler, R., Wehland, J., and Gertler, F.B. (2000). Negative regulation of fibroblast motility by Ena/VASP proteins. Cell *101*, 717–728.

Bear, J.E., Svitkina, T.M., Krause, M., Schafer, D.A., Loureiro, J.J., Strasser, G.A., Maly, I.V., Chaga, O.Y., Cooper, J.A., Borisy, G.G., and Gertler, F.B. (2002). Antagonism between Ena/VASP proteins and actin filament capping regulates fibroblast motility. Cell *109*, 509–521.

Borisy, G.G., and Svitkina, T.M. (2000). Actin machinery: pushing the envelope. Curr. Opin. Cell Biol. *12*, 104–112.

Brummelkamp, T.R., Bernards, R., and Agami, R. (2002). A system for stable expression of short interfering RNAs in mammalian cells. Science *296*, 550–553.

Carlier, M.F. (1998). Control of actin dynamics. Curr. Opin. Cell Biol. *10*, 45–51.

Chou, J., Stolz, D.B., Burke, N.A., Watkins, S.C., and Wells, A. (2002). Distribution of gelsolin and phosphoinositol 4,5-bisphosphate in lamellipodia during EGF-induced motility. Int. J. Biochem. Cell Biol. *34*, 776–790.

Cooper, J.A., and Schafer, D.A. (2000). Control of actin assembly and disassembly at filament ends. Curr. Opin. Cell Biol. *12*, 97–103.

Cooper, J.A., Hart, M.C., Karpova, T.S., and Schafer, D.A. (1999).

Guidebook to the cytoskeletal and motor proteins, 2nd ed. (Oxford: Oxford University Press).

Evangelista, M., Zigmond, S., and Boone, C. (2003). Formins: signaling effectors for assembly and polarization of actin filaments. J. Cell Sci. *116*, 2603–2611.

Grevengoed, E.E., Fox, D.T., Gates, J., and Peifer, M. (2003). Balancing different types of actin polymerization at distinct sites: roles for Abelson kinase and Enabled. J. Cell Biol. *163*, 1267–1279.

Han, Y.H., Chung, C.Y., Wessels, D., Stephens, S., Titus, M.A., Soll, D.R., and Firtel, R.A. (2002). Requirement of a vasodilator-stimulated phosphoprotein family member for cell adhesion, the formation of filopodia, and chemotaxis in dictyostelium. J. Biol. Chem. *277*, 49877–49887.

Harris, E.S., Li, F., and Higgs, H.N. (2004). The mouse formin, FRL-alpha, slows actin filament barbed end elongation, competes with capping protein, accelerates polymerization from monomers, and severs filaments. J. Biol. Chem. *19*, 20076–20087.

Hopmann, R., Cooper, J.A., and Miller, K.G. (1996). Actin organization, bristle morphology, and viability are affected by actin capping protein mutations in Drosophila. J. Cell Biol. *133*, 1293–1305.

Hug, C., Jay, P.Y., Reddy, I., McNally, J.G., Bridgman, P.C., Elson, E.L., and Cooper, J.A. (1995). Capping protein levels influence actin assembly and cell motility in dictyostelium. Cell *81*, 591–600.

Jacinto, A., and Wolpert, L. (2001). Filopodia. Curr. Biol. *11*, R634.

Jung, G., Remmert, K., Wu, X., Volosky, J.M., and Hammer, J.A., 3rd. (2001). The Dictyostelium CARMIL protein links capping protein and the Arp2/3 complex to type I myosins through their SH3 domains. J. Cell Biol. *153*, 1479–1497.

Katoh, K., Hammar, K., Smith, P.J., and Oldenbourg, R. (1999). Birefringence imaging directly reveals architectural dynamics of filamentous actin in living growth cones. Mol. Biol. Cell *10*, 197–210.

Kojima, S., Vignjevic, D., and Borisy, G.G. (2004). Improved silencing vector co-expressing GFP and small hairpin RNA. Biotechniques *36*, 74–79.

Kureishy, N., Sapountzi, V., Prag, S., Anilkumar, N., and Adams, J.C. (2002). Fascins, and their roles in cell structure and function. Bioessays *24*, 350–361.

Kwiatkowski, D.J. (1999). Functions of gelsolin: motility, signaling, apoptosis, cancer. Curr. Opin. Cell Biol. *11*, 103–108.

Kwiatkowski, A.V., Gertler, F.B., and Loureiro, J.J. (2003). Function and regulation of Ena/VASP proteins. Trends Cell Biol. *13*, 386–392.

Lanier, L.M., Gates, M.A., Witke, W., Menzies, A.S., Wehman, A.M., Macklis, J.D., Kwiatkowski, D., Soriano, P., and Gertler, F.B. (1999). Mena is required for neurulation and commissure formation. Neuron *22*, 313–325.

Lebrand, C., Dent, E.W., Strasser, G.A., Lanier, L.M., Krause, M., Svitkina, T.M., Borisy, G.G., and Gertler, F.B. (2004). Critical role of Ena/VASP proteins for filopodia formation in neurons and in function downstream of netrin-1. Neuron *42*, 37–49.

Loisel, T.P., Boujemaa, R., Pantaloni, D., and Carlier, M.F. (1999). Reconstitution of actin-based motility of Listeria and Shigella using pure proteins. Nature *401*, 613–616.

Loureiro, J.J., Rubinson, D.A., Bear, J.E., Baltus, G.A., Kwiatkowski, A.V., and Gertler, F.B. (2002). Critical roles of phosphorylation and actin binding motifs, but not the central proline-rich region, for Ena/vasodilator-stimulated phosphoprotein (VASP) function during cell migration. Mol. Biol. Cell *13*, 2533–2546.

Lu, M., Witke, W., Kwiatkowski, D.J., and Kosik, K.S. (1997). Delayed retraction of filopodia in gelsolin null mice. J. Cell Biol. *138*, 1279–1287.

Mallavarapu, A., and Mitchison, T. (1999). Regulated actin cytoskeleton assembly at filopodium tips controls their extension and retraction. J. Cell Biol. *146*, 1097–1106.

Moseley, J.B., Sagot, I., Manning, A.L., Xu, Y., Eck, M.J., Pellman, D., and Goode, B.L. (2004). A conserved mechanism for Bni1- and mDia1-induced actin assembly and dual regulation of Bni1 by Bud6 and profilin. Mol. Biol. Cell *15*, 896–907.

Mullins, R.D., Heuser, J.A., and Pollard, T.D. (1998). The interaction of Arp2/3 complex with actin: nucleation, high affinity pointed end capping, and formation of branching networks of filaments. Proc. Natl. Acad. Sci. USA *95*, 6181–6186.

Pollard, T.D., and Borisy, G.G. (2003). Cellular motility driven by assembly and disassembly of actin filaments. Cell *112*, 453–465.

Pruyne, D., Evangelista, M., Yang, C., Bi, E., Zigmond, S., Bretscher, A., and Boone, C. (2002). Role of formins in actin assembly: nucleation and barbed-end association. Science *297*, 612–615.

Remmert, K., Olszewski, T.E., Bowers, M.B., Dimitrova, M., Ginsburg, A., and Hammer, J.A., 3rd. (2004). CARMIL is a bona fide capping protein interactant. J. Biol. Chem. *279*, 3068–3077.

Rogers, S.L., Wiedemann, U., Stuurman, N., and Vale, R.D. (2003). Molecular requirements for actin-based lamella formation in Drosophila S2 cells. J. Cell Biol. *162*, 1079–1088.

Rorth, P. (2003). Communication by touch: role of cellular extensions in complex animals. Cell *112*, 595–598.

Rottner, K., Behrendt, B., Small, J.V., and Wehland, J. (1999). VASP dynamics during lamellipodia protrusion. Nat. Cell Biol. *1*, 321–322.

Schafer, D.A., and Cooper, J.A. (1995). Control of actin assembly at filament ends. Annu. Rev. Cell Dev. Biol. *11*, 497–518.

Schafer, D.A., Mooseker, M.S., and Cooper, J.A. (1992). Localization of capping protein in chicken epithelial cells by immunofluorescence and biochemical fractionation. J. Cell Biol. *118*, 335–346.

Schafer, D.A., Korshunova, Y.O., Schroer, T.A., and Cooper, J.A. (1994). Differential localization and sequence analysis of capping protein beta-subunit isoforms of vertebrates. J. Cell Biol. *127*, 453–465.

Schafer, D.A., Jennings, P.B., and Cooper, J.A. (1996). Dynamics of capping protein and actin assembly in vitro: uncapping barbed ends by polyphosphoinositides. J. Cell Biol. *135*, 169–179.

Schafer, D.A., Welch, M.D., Machesky, L.M., Bridgman, P.C., Meyer, S.M., and Cooper, J.A. (1998). Visualization and molecular analysis of actin assembly in living cells. J. Cell Biol. *143*, 1919–1930.

Sizonenko, G.I., Karpova, T.S., Gattermeir, D.J., and Cooper, J.A. (1996). Mutational analysis of capping protein function in Saccharomyces cerevisiae. Mol. Biol. Cell *7*, 1–15.

Strasser, G.A., Rahim, N.A., VanderWaal, K.E., Gertler, F.B., and Lanier, L.M. (2004). Arp2/3 is a negative regulator of growth cone translocation. Neuron *43*, 81–94.

Svitkina, T.M., and Borisy, G.G. (1998). Correlative light and electron microscopy of the cytoskeleton of cultured cells. Methods Enzymol. *298*, 570–592.

Svitkina, T.M., and Borisy, G.G. (1999). Arp2/3 complex and actin depolymerizing factor/cofilin in dendritic organization and treadmilling of actin filament array in lamellipodia. J. Cell Biol. *145*, 1009–1026.

Svitkina, T.M., Bulanova, E.A., Chaga, O.Y., Vignjevic, D.M., Kojima, S., Vasiliev, J.M., and Borisy, G.G. (2003). Mechanism of filopodia initiation by reorganization of a dendritic network. J. Cell Biol. *160*, 409–421.

Taoka, M., Ichimura, T., Wakamiya-Tsuruta, A., Kubota, Y., Araki, T., Obinata, T., and Isobe, T. (2003). V-1, a protein expressed transiently during murine cerebellar development, regulates actin polymerization via interaction with capping protein. J. Biol. Chem. *278*, 5864–5870.

Vignjevic, D., Yarar, D., Welch, M.D., Peloquin, J., Svitkina, T., and Borisy, G.G. (2003). Formation of filopodia-like bundles in vitro from a dendritic network. J. Cell Biol. *160*, 951–962.

von Bulow, M., Rackwitz, H.R., Zimbelmann, R., and Franke, W.W. (1997). CP beta3, a novel isoform of an actin-binding protein, is a component of the cytoskeletal calyx of the mammalian sperm head. Exp. Cell Res. *233*, 216–224.

Zigmond, S.H., Evangelista, M., Boone, C., Yang, C., Dar, A.C., Sicheri, F., Forkey, J., and Pring, M. (2003). Formin leaky cap allows elongation in the presence of tight capping proteins. Curr. Biol. *13*, 1820–1823.